International Journal of Pharmacology

ISSN 1811-7775

science alert

ansinet
Asian Network for Scientific Information

OPEN ACCESS International Journal of Pharmacology

ISSN 1811-7775
DOI: 10.3923/ijp.2025.92.102

Research Article
Therapeutic Effects of *Marasmius androsaceus* Ethanolic Extract on Discogenic Low Back Pain under Mediation of VEGF/VEGFR2 Signaling Pathway

[1]Wanrong Luo, [2]Ying Hong, [1]Xisan Wang, [1]Weihong Yi and [1]Weiqun Lai

[1]Department of Spine Surgery, Huazhong University of Science and Technology Union Hospital Shenzhen, Shenzhen, 518052, Guangdong, China
[2]Department of Ultrasound, Nanshan University of Science and Technology Hospital, Shenzhen, 518052, Guangdong, China

Abstract

Background and Objective: *Marasmius androsaceus*, a common traditional Chinese fungus, has been extensively employed in the preparation of analgesic medications like Anluo Tong for various neuralgia and rheumatoid arthritis treatments. This research studied the Therapeutic Effects of *Marasmius androsaceus* Ethanolic Extract on Discogenic Low Back Pain Under the Mediation of VEGF/VEGFR2 Signaling Pathway. **Materials and Methods:** Active constituents were extracted from *Marasmius androsaceus* fungi. Male Sprague-Dawley (SD) rats were chosen as experimental subjects. A DLBP rat model was created using X-ray-guided puncture. Rats were intervened with 250, 500 and 1,000 mg/kg of MAEE (hereinafter referred to L-MAEE, M-MAEE and H-MAEE groups, respectively). Behavioral characteristics, mechanical withdrawal threshold (MWT), thermal withdrawal latency (TWL), VEGF/VEGFR2 expression and extracellular Regulated Protein Kinases (ERK)/c-Jun N-terminal kinase (JNK)/Mitogen-Activated Protein Kinase (MAPK) protein expression were analyzed. **Results:** In contrast to the DLBP group, L-MAEE, M-MAEE and H-MAEE groups demonstrated reduced gait scores, prolonged hot plate retention time, tail-flick duration and tail-bending duration, showing obvious differences ($p<0.05$). The VEGF and VEGFR2 in IDS cells decreased greatly ($p<0.05$), as did the p-ERK, p-JNK and p-p38 MAPK ($p<0.05$). These effects demonstrated a dose-dependent pattern. **Conclusion:** The MAEE exhibited a dose-dependent alleviation of mechanical hypersensitivity and thermal hyperalgesia in the DLBP animal model. It also ameliorated behavioral changes caused by pain, likely through inhibition of VEGF/VEGFR2 signaling pathway (SPW) and reduction of ERK/JNK/MAPK phosphorylation.

Key words: *Marasmius androsaceus* ethanolic extract, discogenic low back pain, behavioral changes, vascular endothelial growth factor

Citation: Luo, W., Y. Hong, X. Wang, W. Yi and W. Lai, 2025. Therapeutic effects of *Marasmius androsaceus* ethanolic extract on discogenic low back pain under mediation of VEGF/VEGFR2 signaling pathway. Int. J. Pharmacol., 21: 92-102.

Corresponding Author: Ying Hong, Department of Ultrasound, Nanshan University of Science and Technology Hospital, Shenzhen, 518052, Guangdong, China

Funding: This work was supported by Shennanke [2020] Nanshan District Health Technology Plan (Project No. 2020142).

Competing Interest: The authors have declared that no competing interest exists.

Data Availability: All relevant data are within the paper and its supporting information files.

INTRODUCTION

Back pain is a highly prevalent condition in the musculoskeletal system, with approximately 50% of chronic back pain cases being attributed to intervertebral disc degeneration, specifically known as discogenic low back pain (DLBP)[1,2]. Following intervertebral disc degeneration, the rupture and loosening of the fibrous ring can disrupt the stability of the disc. As pressure is applied, the disc gradually shrinks and thins, causing the intervertebral space to narrow. Consequently, the nucleus pulposus migrates towards the fissured fibrous ring, leading to nerve irritation and the onset of pain[3-5].

Since ancient times, herbal medicine has played a significant role as a valuable natural resource within the realm of traditional Chinese medicine (TCM). As research on natural herbs continues to deepen, an increasing number of herbal extracts are gaining widespread attention due to their potential medicinal value. *Marasmius androsaceus*, indigenous to regions such as Yunnan, China, has been a commonly used medicinal herb for hundreds of years in TCM practice. Widely cited in classical herbal literature, *Marasmius androsaceus* has been applied for conditions like pneumonia and cancer, drawing attention to its unique medicinal properties and prompting investigations into its bioactive constituents. The extracts of *Marasmius androsaceus* are believed to have various pharmacological activities, suggesting promising prospects in contemporary pharmaceutical research. The preparation Anluo Tong, primarily consisting of *Marasmius androsaceus* extract, demonstrates analgesic properties and is commonly employed in the treatment of injuries, trigeminal neuralgia, migraines and fracture-related pain[6,7]. Currently, there is relatively limited research on the pharmacological effects of *Marasmius androsaceus* ethanolic extract (MAEE). However, most fungal extracts exhibit multiple pharmacological activities. Fungal extracts contain anti-inflammatory agents that alleviate inflammation and consequently reduce pain resulting from inflammatory reactions[8]. Moreover, fungal extracts can regulate immune system function, enhancing overall immunity[9]. These extracts are also rich in antioxidant constituents such as glutathione and vitamin C, capable of neutralizing free radicals and mitigating oxidative stress-induced damage to the body[10]. Fungal extracts rich in active components such as polysaccharides, triterpenoids and peptides can alleviate pain by modulating neurotransmitters and inhibiting inflammatory responses, thus offering potential analgesic effects[11].

This research assessed the analgesic effects of MAEE on an animal model of DLBP and investigated its underlying mechanisms. It was to offer insights into pain-relieving effects of MAEE on neuropathic pain and offer a reference for the development of treatments for DLBP.

MATERIALS AND METHODS

Study area: The research was performed at Huazhong University of Science and Technology Union Hospital Shenzhen from November, 2022 to October, 2023.

Preparation and detection of MAEE: *Marasmius androsaceus* fungus (China Center for Type Culture Collection of Microorganisms) and its culture medium were extracted by adding 80% ethanol at a 5-fold volume ratio. The mixture was refluxed at 70°C for 1 hr and the residue was filtered repeatedly. This extraction process was repeated until the liquid turned colorless. The combined extract was obtained after ethanol recovery, followed by freeze-drying to yield MAEE. For the control sample, *Marasmius androsaceus* alcohol control was dissolved in distilled water, followed by the addition of a methanol solution and NaOH solution and the mixture was thoroughly mixed. The reaction was carried out in a 70°C water bath for 30 min, followed by cooling for 10 min. The pH was adjusted by adding HCl. The water layer was separated after chloroform extraction in equal volume and the aqueous phase was obtained after overnight settling to obtain the control sample.

The detection of MAEE and the control sample was conducted using liquid chromatography (Shimadzu Corporation, China). A 5 µm XDB-C18 column with dimensions of 4.6×250 mm was utilized. The column temperature, wavelength and flow rate were 40°C, 250 nm and 0.8 mL/min, respectively. The mobile phase consisted of a mixture of 0.025 mol/L PBS and acetonitrile, with a ratio of 85:15 for mobile phase A and 60:40 for mobile phase B. The gradient elution steps were as follows: From 0 to 10 min, a shift from 100 to 92% for A and from 0 to 10% for B; from 10 to 30 min, a change from 92 to 70% for A and from 10 to 30% for B; from 30 to 40 min, a transition from 70 to 65% for A and from 30 to 25% for B and from 40 to 50 min, a progression from 65 to 0% for A and from 25 to 0% for B.

Animals: Fifty rats (Hunan Slake Jingda Laboratory Animal Co., Ltd., China) were of clean status and had an average body weight ranging from 220 to 250 g. They were provided with *ad libitum* access to food and water and were maintained at

a room temperature of approximately 23°C with a relative humidity of about 50%. The rats underwent a 7 day acclimatization period to the laboratory environment before the commencement of the study. All feeding protocols and experimental protocols were conducted in compliance with the guidelines established by the Animal Care and Use Committee.

Construction of DLBP animal model: Anesthesia of the rats was performed using 3% pentobarbital sodium (Sigma-Aldrich, USA) at 0.15 mL/100 g. Forty rats were randomly positioned on their right side for immobilization. Following local disinfection with 75% alcohol, a lateral approach was taken and under X-ray (Shanghai Zhibei Biotechnology Co., Ltd., China) fluoroscopy guidance, a 26G puncture needle was inserted at a 45 degree angle to the horizontal plane and half a finger's width above the spinous process. Needling was conducted separately for the L4~5 and L5~6 intervertebral discs, with exploration of the needle tip until encountering a gritty sensation. Under fluoroscopic guidance, the needle was advanced into the intervertebral disc after which it was rotated 360°. Subsequently, 2.5 µL of sterile phosphate buffer was injected and the needle was left in place for 30 sec before removal. For the sham group, consisting of the remaining 10 rats, the same puncture point was used, but the needle was not inserted into the intervertebral disc.

The remaining 40 DLBP model rats were randomly grouped into four: The DLBP, L-MAEE, M-MAEE and H-MAEE group average. In the DLBP group, rats were administered an equivalent volume of physiological saline after modeling. Rats in L-MAEE, M-MAEE and H-MAEE groups received 250, 500 and 1,000 mg/kg of MAEE, respectively, after modeling. All rats received consecutive doses for 7 days.

Behavioral analysis: On days 1, 3, 7 and 14 following the treatment, behavioral analyses of the rats were conducted. Rats were placed on an animal experimental platform to acclimate for 5 min. Subsequently, the gait changes during rat movement were observed and scored[12]. A score of 3 indicated severe motor impairment with inability to walk, 2 indicated moderate motor impairment with limping walking, 1 indicated mild motor impairment with limping and 0 indicated normal limb movement/activity. For the hot plate test, rats were placed on a 55°C hot plate enclosed by transparent walls to restrict movement. The stopwatch was stopped and the time was recorded when the rat displayed behaviors such as licking the hind paw, shaking the hind paw or jumping within 20 sec. This test was repeated at 10 min intervals. In the tail suspension test, the rats' tails were fixed on a string one-third from the end and they were suspended upside-down on a metal rod located 30 cm above the ground, surrounded by wooden panels to prevent interference. The duration of struggling and bending over within 5 min was recorded.

Pain threshold determination: The rats were placed in a metal mesh cage located above the ground for a 10 min pre-adaptation period. Mechanical stimulation was administered to the sole of the left hind paw using the Von-Frey filament (Shanghai Yuyan Scientific Instrument Co., Ltd., China) with varying forces. The filament was gradually pressed onto the plantar surface of paw until it bent and this pressure was maintained for 5 sec. Starting from 1.0 g, the force of the Von-Frey filament was increased gradually and when the rat displayed a withdrawal reflex, the force was recorded. The pain thresholds were measured at intervals and the mean force was determined as the mechanical withdrawal threshold (MWT). For the thermal stimulation test, by the Hargreaves method[13], the left hind paw of the rats was stimulated using a radiant heat source (Beijing Zhongshi Chuangke Technology Co., Ltd., China). The heat stimulus intensity was set at 35% and the stimulus was automatically cut off after 20 sec. The time taken for the rat to exhibit a withdrawal response was recorded. The pain thresholds were measured at intervals and the mean response time was calculated as the thermal withdrawal latency (TWL).

Immunofluorescence staining: After a 7 week treatment period, lumbar spinal tissues were collected from each group of rats. Anesthesia was induced using 3% pentobarbital sodium at 0.15 mL/100 g. Following disinfection, a fixation was performed by perfusing the heart with 30 mL of 4% paraformaldehyde (Sigma-Aldrich, USA). The rats were positioned in a prone position, with a midline incision along its back. The lumbar 1 to sacral 1 segment was extracted and divided into two portions, with one in liquid nitrogen and the other used for the extraction of lumbar spinal stem cells. After rinsing the tissues with phosphate buffer, the intervertebral disc tissues were minced and centrifuged in ice-cold phosphate-buffered saline. Following digestion with a mixture of type I and type II collagenase, the cells were centrifuged again. The cells were resuspended, filtered and then implanted into culture bottles. They were cultured continuously for 5 to 7 days before being passed. When the cell fusion rate reached around 95%, following PBS washing three times, cells were then fixed using 4% paraformaldehyde for 30 min at room temperature. After washing the cells with

phosphate buffer, they were permeabilized with 0.2% Triton X-100 for 2 min. Following another wash with phosphate buffer, 5% goat serum was added and the cells were subjected to a 30 min incubation. Primary antibodies against VEGF (1:200) (Abcam, UK) and VEGFR2 (1:200) (Abcam, UK) were added separately and the cells were incubated overnight at 4°C with agitation. After washing, fluorescent secondary antibodies (1:300) were added and the cells were treated with 1 hr incubation. The DAPI (Sigma-Aldrich, USA) working solution was used for nuclear counterstaining. After slide sealing, the expression of VEGF and VEGFR2 was observed under a fluorescence microscope (Shanghai Biaimu Optical Instrument Manufacturing Co., Ltd., China).

Western blotting: Lumbar spinal tissues were retrieved from liquid nitrogen and thoroughly ground. A certain proportion of RIPA (Sigma-Aldrich, USA) was mixed with the tissue, which was homogenized. Protein concentration in the extract was assessed using BCA (Shanghai Beyotime Biotechnology Co., Ltd., China). After SDS-PAGE, the proteins were separated and transferred onto a PVDF membrane, which was subsequently blocked using a solution containing 5% skim milk for 3 hrs. Subsequently, primary antibodies against p-ERK (1:1000) (Abcam, UK), p-JNK (1:1000), p-p38 MAPK (1:1000) (Abcam, UK) and GAPDH (1:1000) (Abcam, UK) were separately added and the membrane was incubated all the night at 4°C. The membrane underwent three washes with Tris-HCl-Tween (TBST), followed by a 2 hrs incubation with secondary antibodies, specifically goat anti-rabbit IgG (1:2000) (Abcam, UK). Afterward, the membrane was subjected to another three washes with TBST. Protein bands were then revealed utilizing an ECL kit. Visualization of the protein bands was accomplished using a gel imaging system (Shanghai Tianneng Technology Co., Ltd., China) and subsequent analysis of the images' gray values was carried out using ImageJ.

Statistical analysis: Data were statistically analyzed employing SPSS 19.0 and were presented as Mean±Standard Deviation. Pairwise comparisons between groups were conducted using the t-test. The $p<0.05$ was considered statistically significant.

RESULTS

Characteristic chromatograms of MAEE: In this research, liquid chromatography analysis was performed on MAEE and the control sample. As depicted in Fig. 1, both the characteristic chromatograms of MAEE and the control sample exhibited five main peaks corresponding to mannitol, galacturonic acid, glucose, galactose and arabinose. The relative retention times for these common peaks in the characteristic chromatograms of MAEE were 1.00, 1.85, 2.07, 2.31 and 2.40, with corresponding relative peak areas of 1.00, 0.38, 0.75, 0.94 and 0.36, respectively.

Impacts of MAEE on behavioral characteristics: This research employed puncture technique to establish the DLBP rat model and evaluated changes in behavioral characteristics among different groups of rats. As demonstrated in Fig. 2a, gait scores of rats in DLBP, L-MAEE, M-MAEE and H-MAEE groups all decreased with the extension of treatment time and those

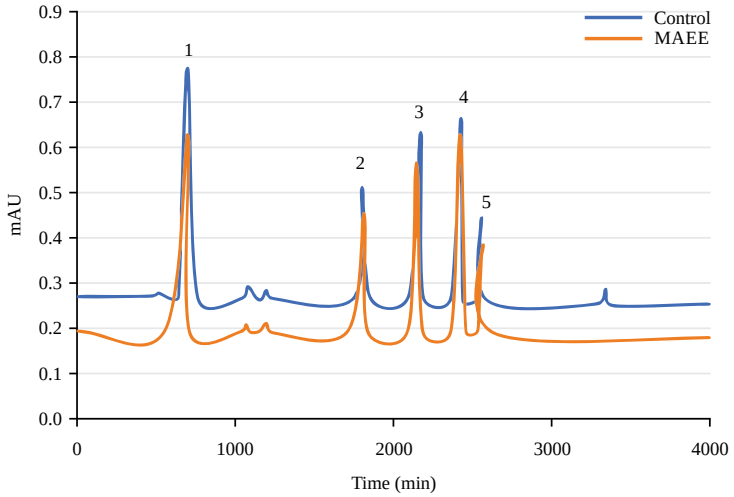

Fig. 1: Characteristic chromatograms of MAEE
1: Mannitol, 2: Galacturonic acid, 3: Glucose, 4: Galactolipid and 5: Arabinose

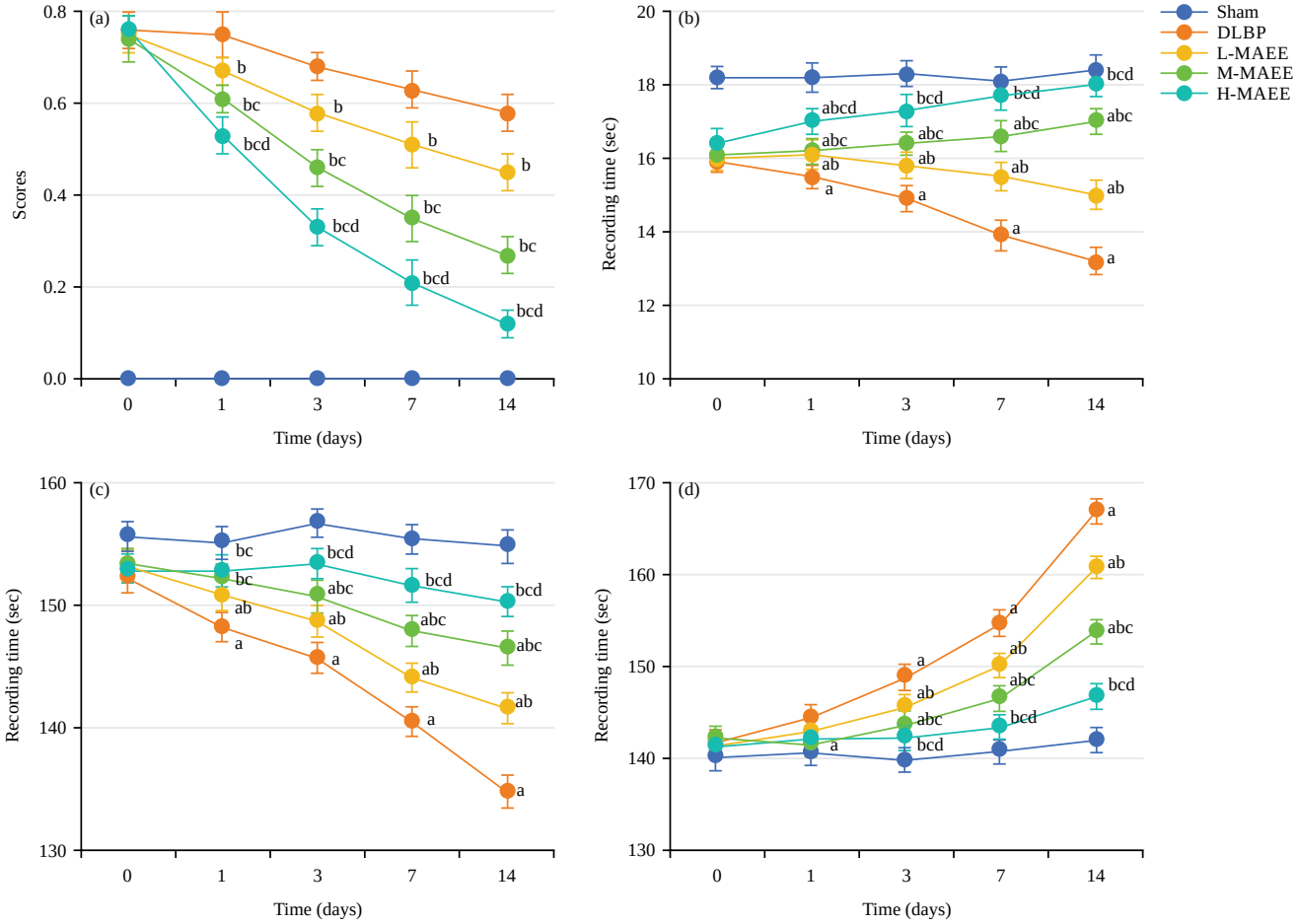

Fig. 2(a-d): Impacts of MAEE on behavioral characteristics of rats, (a) Gait scores, (b) Hot plate retention time, (c) Tail-flick duration and (d) Tail-bending duration

[a]Compared with Sham group, p<0.05; [b]Compared with DLBP group, p<0.05; [c]Compared with L-MAEE group, p<0.05 and [d]Compared with M-MAEE group, p<0.05

in the L-MAEE, M-MAEE and H-MAEE groups remarkably decreased and exhibited obvious differences with the score in DLBP group (p<0.05). In comparison to the L-MAEE group, the gait scores of rats in the M-MAEE and H-MAEE groups also decreased sharply, exhibiting great differences (p<0.05). Moreover, the H-MAEE group exhibited the most obvious reduction in gait scores, demonstrating a significant difference based on the M-MAEE group (p<0.05).

From Fig. 2b, it can be observed that the DLBP group exhibited a remarkable reduction in hot plate retention time in comparison to the Sham, L-MAEE, M-MAEE and H-MAEE groups, with statistically obvious differences (all p<0.05). Moreover, the H-MAEE group had the longest retention time among the three MAEE treatment groups, followed by the M-MAEE group, all demonstrating observable differences with p<0.05.

As explicated in Fig. 2c, the tail-flick duration decreased in the DLBP group based on the Sham and MAEE treatment groups, showing observable differences (p<0.05). Furthermore, relative to the L-MAEE group, tail-flick duration considerably extended in both M-MAEE and H-MAEE groups (p<0.05), with the same trend observed when comparing the M-MAEE with H-MAEE group (p<0.05). As illustrated in Fig. 2d, compared with Sham group, the tail-bending duration was markedly prolonged in the DLBP group, with an obvious difference (p<0.05). Conversely, the tail-bending duration was greatly reduced in three MAEE treatment groups, showing remarkable differences based on the DLBP group (p<0.05). Similarly, compared to L-MAEE group, both the M-MAEE and H-MAEE groups demonstrated a vital reduction in tail-bending duration (p<0.05) and the same pattern persisted when comparing the M-MAEE group with H-MAEE group (p<0.05).

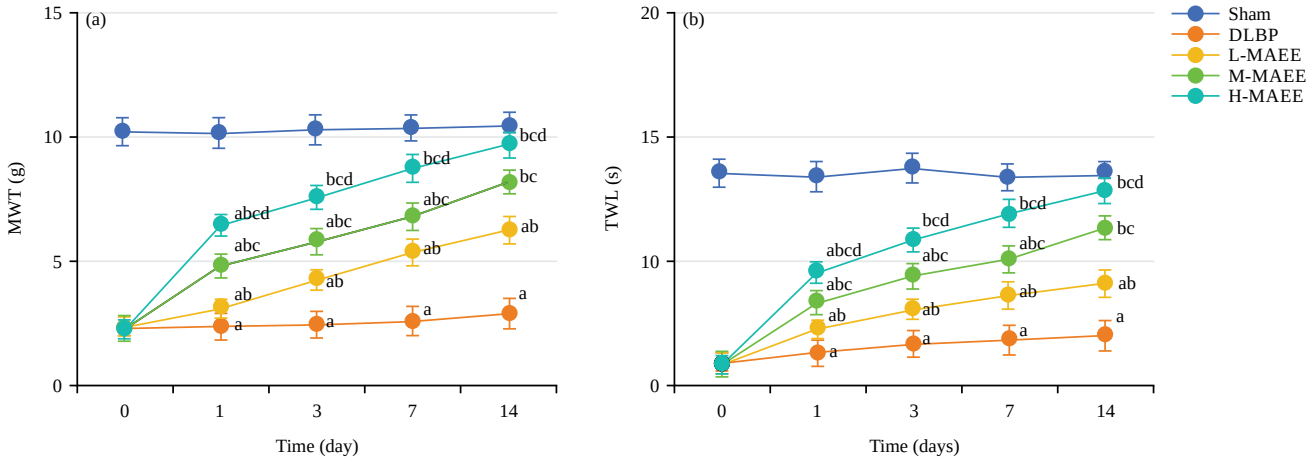

Fig. 3(a-b): Impacts of MAEE on pain of rats, (a) MWT and (b) TWL

[a]Compared with Sham group, p<0.05; [b]Compared with DLBP group, p<0.05; [c]Compared with L-MAEE group, p<0.05 and [d]Compared with M-MAEE group, p<0.05

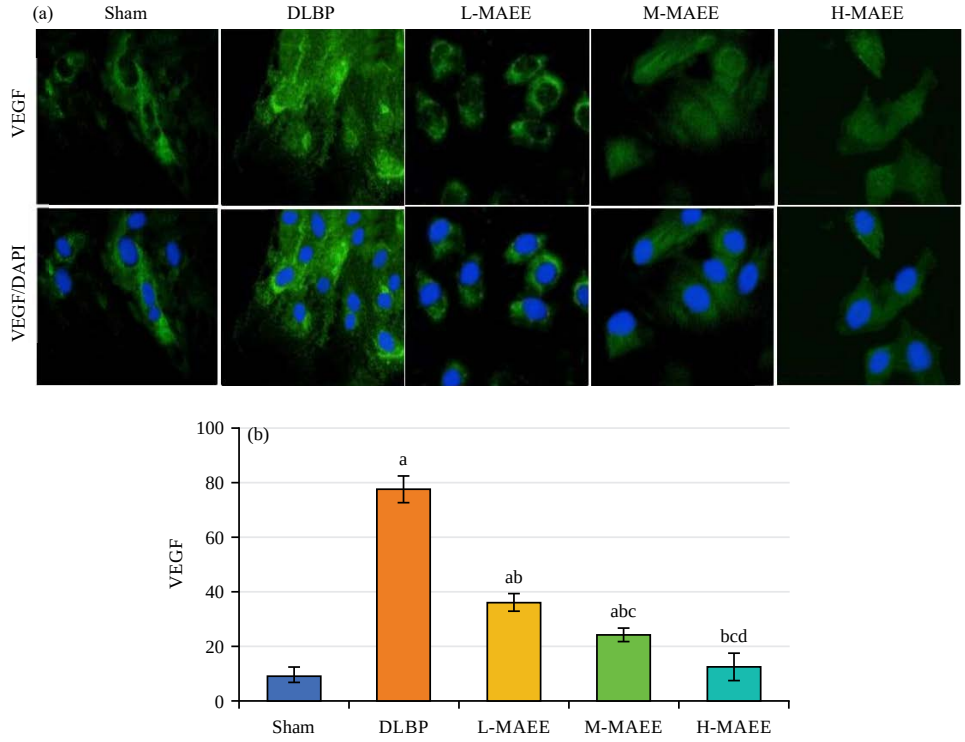

Fig. 4(a-b): VEGF expressions in rats from various groups, (a) Results of immunofluorescence staining (×200) and (b) VEGF expression

[a]Compared with Sham group, p<0.05; [b]Compared with DLBP group, p<0.05; [c]Compared with L-MAEE group, p<0.05 and [d]Compared with M-MAEE group, p<0.05

Impacts of MAEE on pain of rats: This research evaluated changes in pain characteristics among the different groups of rats. As depicted in Fig. 3a-b, rats in the DLBP group experienced lower MWT and TWL values, showing obvious differences with those in the Sham group (p<0.05). In comparison to the DLBP group, rats in three MAEE treatment groups demonstrated a visible increase in both MWT and TWL values, with great differences observed (p<0.05). Furthermore, rats in the L-MAEE and H-MAEE group had the lowest MWT and TWL values, while those in H-MAEE group had the highest values, with p<0.05 for all comparisons.

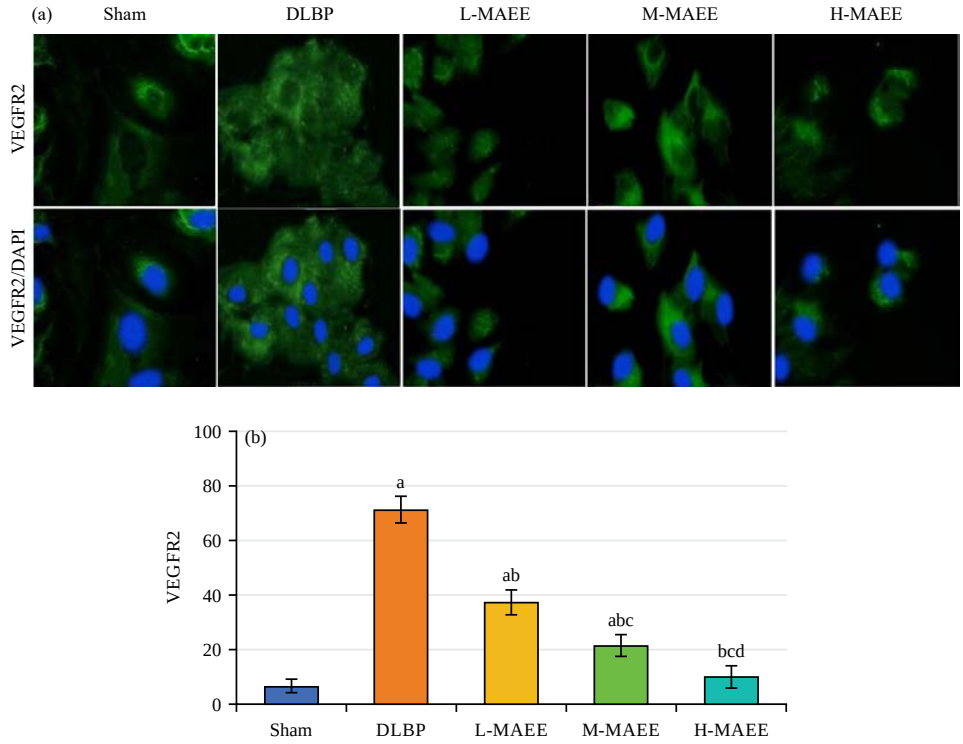

Fig. 5(a-b): Changes in VEGFR2 expressions in rats from various groups, (a) Results of immunofluorescence staining (×200) and (b) VEGFR2 expression

[a]Compared with Sham group, p<0.05; [b]Compared with DLBP group, p<0.05; [c]Compared with L-MAEE group, p<0.05 and [d]Compared with M-MAEE group, p<0.05

Impacts of MAEE on VEGF/VEGFR2 expression: In this research, the differences in VEGF expression in IDS cells among the different rat groups were assessed, as illustrated in Fig. 4 (Fig. 4a shows fluorescent staining of VEGF, while Fig. 4b compares the relative expression of VEGF in intervertebral disc cells among the groups of rats). The DLBP group exhibited elevated VEGF expression in comparison to the Sham and MAEE treatment groups, all demonstrating remarkable differences with p<0.05. Furthermore, rats treated by L-MAEE had the lowest VEGF expression, followed by those intervened by M-MAEE, so rats after H-MAEE intervention experienced the most obviously upregulated VEGF expression, with p<0.05 for all comparisons here.

Figure 5a shows fluorescent staining observation of VEGFR2, while Fig. 5b compares the relative expression of VEGFR2 in intervertebral disc cells among the groups of rats, below displays the differences in VEGFR2 expression in IDS cells among the distinct rat groups. As depicted, based on the Sham group, rats in DLBP group experienced higher VEGFR2 expression (p<0.05) and similar results were observed when comparing those between DLBP group and MAEE intervention groups. Furthermore, the highest and lowest VEGFR2 expressions were visualized in the L-MAEE and H-MAEE groups, respectively, showing remarkable differences with p<0.05.

Impacts of MAEE on expressions of ERK/JNK/MAPK-related proteins: This research assessed changes in expressions of ERK/JNK/MAPK-related proteins in the spinal columns of rats from different groups. As displayed in Fig. 6 (Fig. 6a shows Western blot observation, while Fig. 6b-d, respectively compare the relative expression of p-ERK, p-JNK and p-p38 MAPK in the spinal columns of rats among the groups), rats p-ERK, p-JNK and p-p38 MAPK were upshifted in DLBP group and exhibited obvious differences from those in Sham group (p<0.05). Meanwhile, similar outcomes were observed in comparing those in the DLBP group with those in MAEE intervention groups, showing remarkable significances with p<0.05. Furthermore, the L-MAEE and H-MAEE groups had the maximal and minimal expressions in these proteins, demonstrating significant differences with (p<0.05).

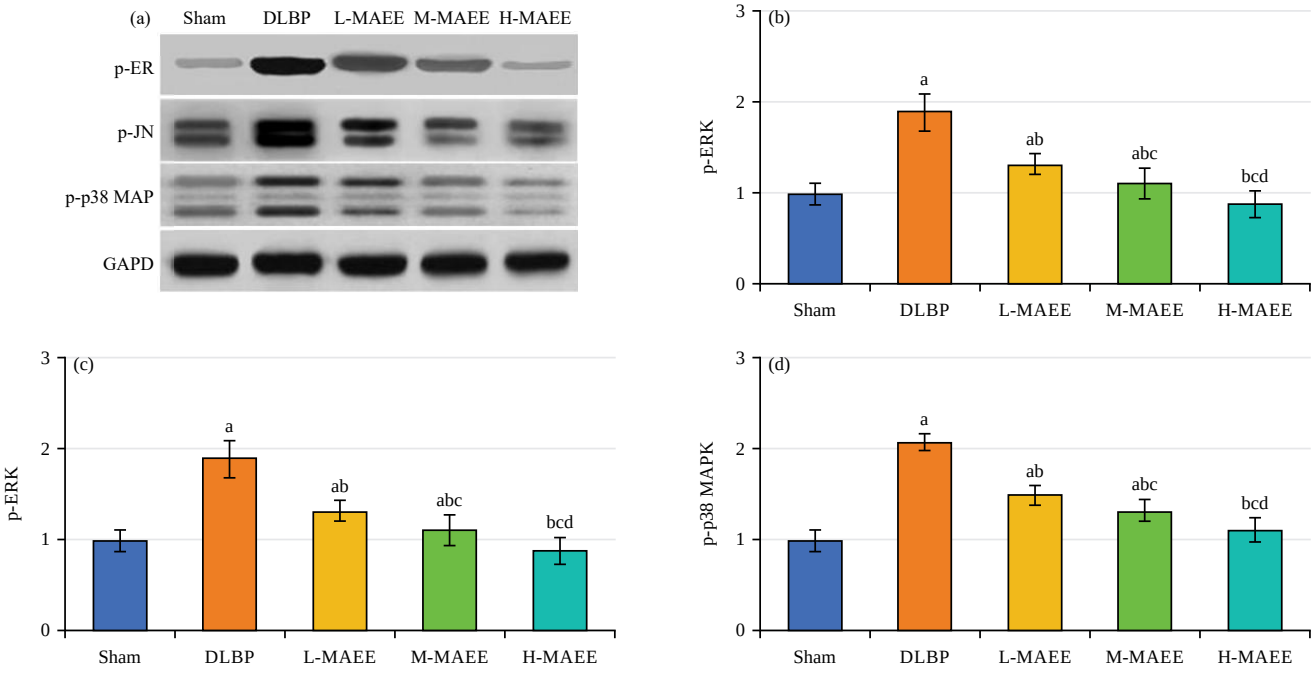

Fig. 6(a-d): Expressions of related proteins, (a) Western blot results, (b) p-ERK, (c) p-JNK and (d) p-p38 MAPK

[a]Compared with Sham group, $p<0.05$; [b]Compared with DLBP group, $p<0.05$; [c]Compared with L-MAEE group, $p<0.05$ and [d]Compared with M-MAEE group, $p<0.05$

DISCUSSION

Based on the animal model, this study investigated the therapeutic effect of MAEE in treating discogenic low back pain and its effect through the VEGF/VEGFR2 signaling pathway. The results showed that the gait score of rats with different concentrations of MAEE was decreased, the hot plate holding time was prolonged and the tail twitch time and tail bending time were significantly increased. The expression levels of VEGF, VEGFR2, p-ERK, p-JNK and p-p38 MAPK proteins were decreased. It is suggested that MAEE may alleviate mechanical hypersensitivity and heat pain in the model of discogenic low back pain by inhibiting the VEGF/VEGFR2 signaling pathway reducing the ERK/JNK/MAPK phosphorylation mechanism and improving the behavioral changes caused by pain.

Penetration modeling techniques are commonly employed in the construction of DLBP animal models due to their convenience, minimal invasiveness and controllable penetration depth[14,15]. Based on the advantages of this modeling method, a rat model of discogenic low back pain was constructed. Studies have shown that DLBP often presents as groin and thigh nerve root pain, as well as lumbago symptom[16]. The results showed that the duration of DLBP rats on the hot plate was significantly reduced, indicating a decreased tolerance to heat pain stimulation. This is attributed to factors such as sensitization of peripheral nerve fibers following pathological changes in intervertebral discs[17]. In this experiment, the results showed that after MAEE treatment, the gait score of rats was decreased, the hot plate holding time was prolonged and the tail twitch time and tail bending time were significantly increased. It suggested that MAEE treatment could significantly improve the behavioral characteristics of DLBP rats in a dose-dependent manner. After MAEE treatment, the rats had a longer response time to painful tail stimuli, indicating a reduction in pain perception or an enhanced analgesic effect. The same change in tail bending time can reflect the sensitivity of rats to painful stimuli and the effect of pain relief. These results all suggest that MAEE has analgesic effects. *Marasmius androsaceus* is a medicinal fungus with antihypertensive, analgesic and antioxidant properties[18-20]. Song *et al.*[21] pointed out that *Marasmius androsaceus* ethanol (MAE) extract has a significant analgesic effect and its analgesic effect is related to the metabolic regulation of monoamine neurotransmitters and the Ca^{2+}/CaMKII-mediated signaling pathway. Herbal medicines such as Tongning and Anluotone, primarily prepared using *Marasmius androsaceus* as the main ingredient, are widely used for analgesic treatment and have demonstrated significant therapeutic efficacy[22]. The Chinese

patent medicine Anluotone, primarily prepared using MAEE, is commonly used for pain and inflammation relief associated with rheumatoid arthritis, musculoskeletal pain and soft tissue injuries. This medication acts by suppressing inflammatory responses and alleviating pain. The results of this study are similar to those of the above studies, indicating that *Marasmius androsaceus* extract has significant analgesic effects.

The VEGF plays a crucial role in the degeneration of lumbar intervertebral discs[23,24]. The VEGF promotes angiogenesis and improves tissue blood supply[25], thereby participating in the process of disc regeneration and repair[26]. In healthy and mature intervertebral disc tissues during growth and development, VEGF expression levels are low. However, after disc degeneration occurs, VEGF expression levels become abnormally elevated, increasing with the severity of disc degeneration[27]. During the process of degenerative disc disease, excessive expression of VEGF can lead to abnormal blood vessel formation, triggering inflammation around the intervertebral disc and causing pain[28].

In this study, differences in VEGF expression levels in intervertebral disc stem cells among rat groups were evaluated, revealing a significant decrease in VEGF expression levels after MAEE treatment ($p<0.05$), with a more pronounced effect observed at higher concentrations ($p<0.05$). This indicates that MAEE can exert therapeutic effects on DLBP by inhibiting VEGF expression. However, VEGF plays a dual role in DLBP, where moderate VEGF expression promotes disc repair, while excessive expression exacerbates inflammation and pain development[29]. Therefore, further investigation is needed to elucidate the specific mechanisms of VEGF in DLBP for future therapeutic strategies. Members of the VEGF family signal through tyrosine kinase receptors upon binding. In osteoarthritis, VEGF can bind and activate VEGFR2, leading to cartilage degeneration and the development of osteoarthritis[30]. Study demonstrated that the VEGFR2 inhibitor Vandetanib significantly inhibits the progression of osteoarthritis[31]. In this study, differences in VEGFR2 expression levels in intervertebral disc stem cells among rat groups were assessed, revealing a significant decrease in VEGFR2 expression levels after MAEE treatment ($p<0.05$), with a more pronounced effect observed at higher concentrations ($p<0.05$). The VEGFR2 primarily regulates angiogenesis and vascular permeability[32]. This research indicated that MAEE can exert therapeutic effects on DLBP by inhibiting VEGFR2 expression.

The DLBP is characterized by pain in the lumbar region caused by disc degeneration or injury. Disc degeneration or injury can lead to inflammation and activation of cellular SPWs, thereby activating the ERK/JNK/MAPK pathway[33]. The ERK, JNK and MAPK pathways are intracellular SPWs involved in various biological processes, including pain regulation[34]. Miao *et al.*[35] have confirmed that activation of the ERK, JNK and MAPK SPWs is closely associated with the development and maintenance of pain. Activation of the ERK pathway can promote neuronal sensitization, synaptic plasticity and release of pro-nociceptive substances in the spinal cord and brain[36]. The JNK SPW is involved in inflammation and neuronal apoptosis regulation and its activation is associated with the progression of neuropathic pain[37]. The MAPK pathway includes ERK, JNK and other kinases that integrate various extracellular stimuli and transmit signals in pain pathways at different levels[38]. In this study, changes in spinal ERK/JNK/MAPK-related protein expression levels among rat groups were assessed, revealing a significant decrease in the expression levels of p-ERK, p-JNK and p-p38 MAPK proteins in rats treated with MAEE ($p<0.05$), with a more pronounced effect observed at higher concentrations ($p<0.05$). Activation of the ERK/JNK/MAPK SPW may mediate the release of inflammatory cytokines, increased excitability of neurons and changes in pain transmission, thereby contributing to the occurrence and maintenance of DLBP[39,40]. The MAEE can dose-dependently inhibit the activation of the ERK/JNK/MAPK SPW, thereby improving the severity of pain in DLBP rats.

CONCLUSION

The MAEE contains multiple bioactive components and can improve mechanical pain and TWL in DLBP in a dose-dependent manner, thereby ameliorating behavioral changes in an animal model induced by pain. Its main mechanism of action involved the inhibition of VEGF/VEGFR2 expression and ERK/JNK/MAPK phosphorylation. This research specifically assessed the analgesic effect of MAEE on the DLBP animal model, but further evaluation was needed to understand its impact on degenerative changes in intervertebral discs. In conclusion, MAEE demonstrated analgesic effects on neuropathic pain and neurogenic pain. Further research was required to comprehensively assess its potential therapeutic benefits on intervertebral disc degeneration.

SIGNIFICANCE STATEMENT

Marasmius androsaceus is commonly used in treating various neuralgias and shows excellent efficacy. To understand its therapeutic mechanism for discogenic low back pain, it established a rat model of discogenic low back pain and intervened with *Marasmius androsaceus* ethanol extract treatment. It found that this treatment significantly improved behavioral changes induced by pain in rats and exerted its effects through the VEGF/VEGFR2 pathway.

REFERENCES

1. Isa, I.L.M., S.L. Teoh, N.H.M. Nor and S.A. Mokhtar, 2023. Discogenic low back pain: Anatomy, pathophysiology and treatments of intervertebral disc degeneration. Int. J. Mol. Sci., Vol. 24. 10.3390/ijms24010208.
2. Masood, Z., A.A. Khan, A. Ayyub and R. Shakeel, 2022. Effect of lumbar traction on discogenic low back pain using variable forces. J. Pak. Med. Assoc., 72: 483-486.
3. Huang, Y., L. Wang, B. Luo, K. Yang and X. Zeng *et al*., 2022. Associations of lumber disc degeneration with paraspinal muscles myosteatosis in discogenic low back pain. Front. Endocrinol., Vol. 13. 10.3389/fendo.2022.891088.
4. Urits, I., A. Capuco, M. Sharma, A.D. Kaye, O. Viswanath, E.M. Cornett and V. Orhurhu, 2019. Stem cell therapies for treatment of discogenic low back pain: A comprehensive review. Curr. Pain Headache Rep., Vol. 23. 10.1007/s11916-019-0804-y.
5. Quinones, S., M. Konschake, L.L. Aguilar, C. Simon and P. Aragones *et al*., 2021. Clinical anatomy of the lumbar sinuvertebral nerve with regard to discogenic low back pain and review of literature. Eur. Spine J., 30: 2999-3008.
6. Meng, F., G. Xing, Y. Li, J. Song and Y. Wang *et al*., 2016. The optimization of *Marasmius androsaceus* submerged fermentation conditions in five-liter fermentor. Saudi J. Biol. Sci., 23: S99-S105.
7. Song, J., X. Wang, Y. Huang, Y. Qu, L. Teng, D. Wang and Z. Meng, 2017. Antidepressant-like effects of *Marasmius androsaceus* metabolic exopolysaccharides on chronic unpredictable mild stress-induced rat model. Mol. Med. Rep., 16: 5043-5049.
8. Lee, H.Y., C.C. Chen, C.C. Pi and C.J. Chen, 2023. *Aspergillus oryzae* fermentation extract alleviates inflammation in *Mycoplasma pneumoniae* pneumonia. Molecules, Vol. 28. 10.3390/molecules28031127.
9. Ku, Y.H., J.H. Kang and H. Lee, 2022. Effects of *Phellinus linteus* extract on immunity improvement: A CONSORT-randomized, double-blinded, placebo-controlled trial. Medicine, Vol. 101. 10.1097/MD.0000000000030226.
10. Liang, H.W., T.Y. Yang, C.S. Teng, Y.J. Lee and M.H. Yu *et al*., 2021. Mulberry leaves extract ameliorates alcohol-induced liver damages through reduction of acetaldehyde toxicity and inhibition of apoptosis caused by oxidative stress signals. Int. J. Med. Sci., 18: 53-64.
11. Shen, C.L., R. Wang, G. Ji, M.M. Elmassry and M. Zabet-Moghaddam *et al*., 2022. Dietary supplementation of gingerols- and shogaols-enriched ginger root extract attenuate pain-associated behaviors while modulating gut microbiota and metabolites in rats with spinal nerve ligation. J. Nutr. Biochem., Vol. 100. 10.1016/j.jnutbio.2021.108904.
12. Lee, S.Y., B.D. Schmit, S.N. Kurpad and M.D. Budde, 2022. Acute magnetic resonance imaging predictors of chronic motor function and tissue sparing in rat cervical spinal cord injury. J. Neurotrauma, 39: 1727-1740.
13. Hogri, R., B. Baltov, R. Drdla-Schutting, V. Mussetto, H. Raphael, L. Trofimova and J. Sandkühler, 2023. Probing pain aversion in rats with the "Heat Escape Threshold" paradigm. Mol. Pain, Vol. 19. 10.1177/17448069231156657.
14. Shi, C., V. Das, X. Li, R. Kc and S. Qiu *et al*., 2018. Development of an *in vivo* mouse model of discogenic low back pain. J. Cell. Physiol., 233: 6589-6602.
15. Nojima, D., K. Inage, Y. Sakuma, J. Sato and S. Orita *et al*., 2016. Efficacy of anti-NaV1.7 antibody on the sensory nervous system in a rat model of lumbar intervertebral disc injury. Yonsei Med. J., 57: 748-753.
16. Mohammed, S. and J. Yu, 2018. Platelet-rich plasma injections: An emerging therapy for chronic discogenic low back pain. J. Spine Surg., 4: 115-122.
17. Kallewaard, J.W., C. Edelbroek, M. Terheggen, A. Raza and J.W. Geurts, 2020. A prospective study of dorsal root ganglion stimulation for non-operated discogenic low back pain. Neuromodulation: Technol. Neural Interface, 23: 196-202.
18. Song, J., X. Geng, Y. Su, X. Zhang, L. Tu, Y. Zheng and M. Wang, 2020. Structure feature and antidepressant-like activity of a novel exopolysaccharide isolated from *Marasmius androsaceus* fermentation broth. Int. J. Biol. Macromol., 165: 1646-1655.
19. Zhang, L., M. Yang, Y. Song, Z. Sun, Y. Peng, K. Qu and H. Zhu, 2009. Antihypertensive effect of 3,3,5,5-tetramethyl-4-piperidone, a new compound extracted from *Marasmius androsaceus*. J. Ethnopharmacol., 123: 34-39.
20. Song, J., G. Xing, J. Cao, L. Teng and C. Li *et al*., 2016. Investigation of the antidepressant effects of exopolysaccharides obtained from *Marasmius androsaceus* fermentation in a mouse model. Mol. Med. Rep., 13: 939-946.

21. Song, J., X. Wang, Y. Huang, Y. Qu, G. Zhang and D. Wang, 2018. Analgesic effects of *Marasmius androsaceus* mycelia ethanol extract and possible mechanisms in mice. Braz. J. Med. Biol. Res., Vol. 51. 10.1590/1414-431X20177124.
22. Zhao, J., X. Zeng, J. Liu, X. Liu and Z. Liu *et al*., 2023. *Marasmius androsaceus* mitigates depression-exacerbated intestinal radiation injuries through reprogramming hippocampal miRNA expression. Biomed. Pharmacother., Vol. 165. 10.1016/j.biopha.2023.115157.
23. Ertugrul, B., B. Akgun, G. Artas, F.S. Erol and F. Demir, 2022. Evaluation of BMP-2, VEGF, and vitamin D receptor levels in the ligamentum flavum of patients with lumbar spinal stenosis and disc herniation. Turk. Neurosurg., 32: 91-96.
24. Zhan, J.W., S.Q. Wang, M.S. Feng, J.H. Gao and X. Wei *et al*., 2021. Effects of axial compression and distraction on vascular bud and VEGFA expression in the vertebral endplate of an *ex vivo* rabbit spinal motion segment culture model. SPINE, 46: 421-432.
25. Tian, Y., F. Zhang, Y. Qiu, S. Wang and F. Li *et al*., 2021. Reduction of choroidal neovascularization via cleavable VEGF antibodies conjugated to exosomes derived from regulatory T cells. Nat. Biomed. Eng., 5: 968-982.
26. Aydin, H.E., S. Yigit, I. Kaya, E. Tural, S. Tuncer and A.F. Nursal, 2022. *VEGF* and *eNOS* variants may influence intervertebral disc degeneration. Nucleosides Nucleotides Nucleic Acids, 41: 982-993.
27. Capossela, S., A. Bertolo, K. Gunasekera, T. Pötzel, M. Baur and J.V. Stoyanov, 2018. VEGF vascularization pathway in human intervertebral disc does not change during the disc degeneration process. BMC Res. Notes, Vol. 11. 10.1186/s13104-018-3441-3.
28. Zhang, B., Q. Zhao, Y. Li and J. Zhang, 2019. Moxibustion alleviates intervertebral disc degeneration via activation of the HIF-1α/VEGF pathway in a rat model. Am. J. Transl. Res., 11: 6221-6231.
29. Qiu, S., C. Shi, A.N. Anbazhagan, V. Das and V. Arora *et al*., 2020. Absence of VEGFR-1/Flt-1 signaling pathway in mice results in insensitivity to discogenic low back pain in an established disc injury mouse model. J. Cell. Physiol., 235: 5305-5317.
30. Das, V., R. Kc, X. Li, I. O-Sullivan and A.J. van Wijnen *et al*., 2018. Blockade of vascular endothelial growth factor receptor-1 (Flt-1), reveals a novel analgesic for osteoarthritis-induced joint pain. Gene Rep., 11: 94-100.
31. Nagao, M., J.L. Hamilton, R. Kc, A.D. Berendsen and X. Duan *et al*., 2017. Vascular endothelial growth factor in cartilage development and osteoarthritis. Sci. Rep., Vol. 7. 10.1038/s41598-017-13417-w.
32. Heinolainen, K., S. Karaman, G. D'Amico, T. Tammela and R. Sormunen *et al*., 2017. VEGFR3 modulates vascular permeability by controlling VEGF/VEGFR2 signaling. Circ. Res., 120: 1414-1425.
33. Zhang, J., X. Wang, H. Liu, Z. Li and F. Chen *et al*., 2019. TNF-α enhances apoptosis by promoting chop expression in nucleus pulposus cells: Role of the MAPK and NF-κB pathways. J. Orthop. Res., 37: 697-705.
34. Sanna, M.D., C. Ghelardini and N. Galeotti, 2014. Regionally selective activation of ERK and JNK in morphine paradoxical hyperalgesia: A step toward improving opioid pain therapy. Neuropharmacology, 86: 67-77.
35. Miao, G.S., Z.H. Liu, S.X. Wei, J.G. Luo, Z.J. Fu and T. Sun, 2015. Lipoxin A_4 attenuates radicular pain possibly by inhibiting spinal ERK, JNK and NF-κB/p65 and cytokine signals, but not p38, in a rat model of non-compressive lumbar disc herniation. Neuroscience, 300: 10-18.
36. Kondo, M. and I. Shibuta, 2020. Extracellular signal-regulated kinases (ERK) 1 and 2 as a key molecule in pain research. J. Oral Sci., 62: 147-149.
37. Zhang, L.Q., S.J. Gao, J. Sun, D.Y. Li and J.Y. Wu *et al*., 2022. DKK3 ameliorates neuropathic pain via inhibiting ASK-1/JNK/p-38-mediated microglia polarization and neuroinflammation. J. Neuroinflammation, Vol. 19. 10.1186/s12974-022-02495-x.
38. Kong, F., K. Sun, J. Zhu, F. Li and F. Lin *et al*., 2021. PD-L1 improves motor function and alleviates neuropathic pain in male mice after spinal cord injury by inhibiting MAPK pathway. Front. Immunol., Vol. 12. 10.3389/fimmu.2021.670646.
39. Sun, K., J. Zhu, C. Yan, F. Li and F. Kong *et al*., 2021. CGRP regulates nucleus pulposus cell apoptosis and inflammation via the MAPK/NF-κB signaling pathways during intervertebral disc degeneration. Oxid. Med. Cell. Longevity, Vol. 2021. 10.1155/2021/2958584.
40. Xiao, L., K. Hong, C. Roberson, M. Ding and A. Fernandez *et al*., 2018. Hydroxylated fullerene: A stellar nanomedicine to treat lumbar radiculopathy via antagonizing TNF-α-induced ion channel activation, calcium signaling, and neuropeptide production. ACS Biomater. Sci. Eng., 4: 266-277.